Study Of Structural, Morphological And Electrical Properties Of $Ti_{50}Nb_{50}$ (Ti -66 wt.% Nb) Thin Films On Glass Substrate At Different Temperatures 100°C, 200°C and 300°C

ADITI[1] & Dr. ANAND K. TYAGI[2]
[1]Department of Applied Sciences, I.K.Gujral Punjab Technical University, kapurthla (Punjab), India.
[2]Department of Applied Sciences, SBS State Technical Campus, Firozpur (Punjab), India.

Received: July 23, 2018 Accepted: October 08, 2018

ABSTRACT *In this research, $Ti_{50}Nb_{50}$ (Ti-66 wt.%Nb) alloy films were deposited on glass substrates using RF Sputtering technique. The effect of substrate temperature (100°C, 200°C and 300°C) on time of deposition, structural, morphology and electrical properties of films were examined using X-Ray Diffraction (XRD), Field Emission Scanning Electron Microscopy (FESEM), Atomic Force Microscopy (AFM) and Hall measurements. Results show that with an increase in substrate temperature, the β-Titanium phase is found to involve in Ti-Nb alloy system. Thin films deposited at high substrate temperatures also showed an increase in surface roughness and grain size. The electrical measurements on these films show the higher values of resistivity increase with increase in temperature.*

Keywords: *Ti-Nb alloy, RF Sputtering, Microstructure, Morphological Properties*

INTRODUCTION:

The studies on physical properties of Ti-Nb alloy thin films with different compositions have been the subject of investigations for many years. Many methods such as PVD (Physical Vapour Deposition), CVD (Chemical Vapour Deposition), Sputtering and PLD (pulsed laser deposition) [1-4] have been employed for the fabrication of the alloy thin films in this system. Out of these, sputtering technique is best known because of its high deposition rate, uniformity, homogeneous, density, purity, adhesion, good reproducibility, provision for uniform thickness on large-area substrates and the easy access of commercially available sputtering system to deposit the thin films of high transparency and conductivity [5,6]. Magnetron Sputtering is a simple and low-cost variant of sputtering for obtaining thin films of materials with relatively high value of melting points like metals, alloys, nitrides, carbides or oxides [7].

Niobium based thin films are attractive materials for many important potential applications in modern technology including, electrochromism, catalysis, batteries, solar cells and other electronic devices such as memristors. Niobium is also widely used in many important superconducting applications. At ambient pressure, bulk Nb has the highest critical temperature, Tc ≈ 9.25 K among the superconducting elements. Here it is important to mention that Niobium, like Mo, V, W, Nb and Ta is also a good β-phase stabilizer in Titanium.

Ti based alloying elements can be categorized according to their effect on the stabilities of αTi and βTi phases. Pure titanium has a hexagonal close packed structure known as αTi and the structure of body centered cubic termed as βTi. Alloying these metals with Titanium become βTi alloys. Most α+β alloys have high-strength and formability [8,9]. In addition to strengthening the beta phase, beta stabilisers have important advantages as alloying constituents. Beta titanium has an inherently lower resistance to deformation than the alpha modification and therefore elements which increase and stabilise the beta phase tend to improve alloy fabricability during both hot and cold working operations.

The alloy combinations of Titanium and Niobium up to 60:40 atomic percentages have been tried by researchers; however, there are no reports on Nb rich alloy combinations. We have investigated the Ti-Nb alloy combination of 50:50, hereafter referred as $Ti_{50}Nb_{50}$ (i.e. Ti + 66 wt. % Nb) in the present study. Titanium-Niobium films with above mentioned composition have been deposited on glass substrate by RF magnetron sputtering and deposited films were then characterized mainly for their microstructural evolution features and functional properties by XRD, FESEM, AFM and HALL measurements. The influence of substrate temperature on the morphology; texture, roughness, grain size and electrical properties of the fabricated thin films has also been thoroughly studied in the present work.

EXPERIMENTAL DETAILS:

Deposition:

The Ti-Nb films were deposited by RF magnetron sputtering onto glass substrates using Titanium-Niobium alloy target (50-mm diameter and 3-mm thick) with a minimum purity of 99.9%. The glass substrates were cleaned by rinsing in ultrasonic baths of acetone for 10-15 minutes and dried. Glass substrates were cut into different sizes of requirement and clamped on the substrate holder in the chamber. Vacuum was created in the sputtering chamber not less than 10^{-6} Torr by using a turbo molecular pump. Commercial argon (Ar) gas of 99.9% purity was used as the sputtering gas and it has kept constant at gas flow rate of 15 sccm that can be controlled by a mass flow controller. Base pressure was kept at $8x10^{-6}$mbar and working pressure was 1.7×10^{-2}mbar. In this process target-substrate distance was kept at 7-8 cm. Sputtering rf power was kept constant at 100W. For making thin films of thickness 200nm, the deposition time of the films with same composition of the alloy ($Ti_{50}Nb_{50}$) at different temperatures (100°C, 200°C and 300°C) was analyzed. Table 1 list out the deposition time for $Ti_{50}Nb_{50}$ alloy thin film of 200 nm thickness at different temperatures (100°C, 200°C and 300°C). Deposition time decreases at 200°C and it remains same for 100°C and 300°C.

Table 1: Deposition Time with increase in Substrate Temperature with thickness 200 nm thin film ($Ti_{50}Nb_{50}$) on glass substrate

Temperature	100°C	200°C	300°C
Deposition Time (min)	76	59	78

Characterization:

The synthesized thin film samples were analyzed for phases present by X-Ray Diffractometer (Panalytical X Pert Pro) at 40 kV and 30 mA using a Ni-filtered with Cu K_α (λ = 1.54056 Å) radiation source. The scanning speed was 2°/min and the scanning angle 2θ ranged from 30° to 80°. Phases were identified by matching their characteristic peaks with files of the Joint Committee on Powder Diffraction Standards (JCPDS). The surface topographical characterizations of the Ti-Nb films were obtained from FESEM (Nova Nano FE-SEM 450) (FEI). It provides ultra high resolution characterization & analysis giving precise, true nanometer scale information. It gives a resolution of 1.4 nm at 1 kV (TLD-SE) & 1 nm at 15 kV (TLD-SE). We have done EDX attached with SEM for measuring the elemental chemical composition of materials. Beam landing energy can go down from 30 keV to 50 eV. The surface morphology (AFM) of the Ti films was also characterized by using Multimode Scanning Probe Microscope (Bruker).

RESULTS AND DISCUSSIONS:

X-Ray Diffraction (XRD) Studies:

XRD data was obtained from the Panalytical X Pert Pro for scan 2θ from 30° to 80°. The phases were identified by matching each characteristic peak with the JCPDS files (JCPDS card No.44-1294) [10, 11]. All the studies were carried out on films of approximately the same thickness (3mm). Typical XRD patterns of the films deposited at 100°C, 200°C, and 300°C are shown in Fig 1. As we can see that the films deposited at 100°C showed a single low intensity peak at angle 36.8449° due to (110) reflection. No other XRD peaks corresponding to reflections at (101), (200) and (112) planes of $Ti_{50}Nb_{50}$ were observed in this case, clearly depicting a prominently amorphous nature of this sample. However, films deposited at 200°C, clearly showed the presence of relatively high intensity peaks at (110), (101) and (200) at angle 35.9113°, 41.6245° and 60.2468°. In contrast, the films deposited at higher substrate temperature of 300°C showed peaks with much higher intensity. At 300°C peaks are reported at 35.5770°, 41.2826°, 59.6673° and 71.3954° with miller indices (110), (101), (200) and (112) respectively. These four peaks in X-ray diffraction patterns are polycrystalline in nature deposited on glass substrate [12].

The intensity of these peaks increases with increase in temperature. The preferred orientation is (110) as indicated the strongest diffraction peak as we can see clearly in Fig 1. Other peaks as indicated with much less intensity was observed. The highest peak value of the XRD measurement was obtained from the film deposited at 300°C at an angle 35.5770°. At lower substrate temperature 100°C and 200°Cthe appearance of broad humps in XRD pattern is suggestive of amorphous nature, of these films [13, 14]. In case of 300°C, the films showed crystallinity and distinct film-structure, in spite of similar film-composition. The existence of several diffraction peaks at 300°Cis indication of poly-crystalline nature. It was thus obvious that a higher substrate temperature helped achieving enhanced crystallization.

The crystalline size of thin films $Ti_{50}Nb_{50}$ were determined from the XRD spectra by using Scherrer's formula, where λ, θ and B are the X-ray wavelength (1.54 Å), Bragg diffraction angle and line of full width at half maximum, respectively. The films have the highest peak value of XRD and the narrowest value of FWHM

has the best crystal quality. It was observed that crystalline size increasing from 97.21nm to 113.59 nm with increase in substrate temperature. The increasing crystalline size is due to the emerging of the smaller particles into larger ones resulting from the potential energy difference between small and large particles, which was occur through solid state diffusion. Change in the intensities in XRD is attributed to the crystallinity of the materials. Many times on heat treatment; % crystallinity of the sample increases which further results in the enhancement of XRD peak intensities.

Another interesting feature in XRD profiles of Ti-Nb alloy peaks are shifting towards lower angles. Shifting in peaks is possibly due to increase in d-spacing. Increase in d-spacing is due to difference in ionic radii of Ti and Nb ions. The ionic radii of Nb ions is greater than Ti ions (Ti= 74.5pm and Nb=78pm). Increase in plane spacing (d values) is due to rearrangement of lattice positions. Niobium is a β-stabiliser, so plane (110) is the densest plane of βTi phase which has a body centered cubic structure. Position shift can be related to the change in lattice parameters due to alloying at increasing temperature. Hence it implies that 2θ shifts to lower values and films are becoming more crystalline.

Table 2: Crystallite Size, Lattice Strain and Other XRD Parameters for $Ti_{50}Nb_{50}$ Alloy at 100°C, 200°C and 300°C

Temprature	XRD Peak Position [°2θ]	FWHM (radians)	Crystalline size (nm)	Intensity	d-spacing [Å]
100°C	36.8449	0.0900	97.21	63	2.4375
200°C	35.9113	0.4723	18.48	57.30	2.5007
200°C	41.6245	0.0900	98.67	46	2.1679
200°C	60.2468	0.7085	13.55	26.29	1.5362
300°C	35.5770	0.0900	96.86	70	2.5214
300°C	41.2826	0.0900	98.56	64	2.1851
300°C	59.6673	0.0900	106.33	55	1.5483
300°C	71.3954	0.0900	113.59	51	1.3201

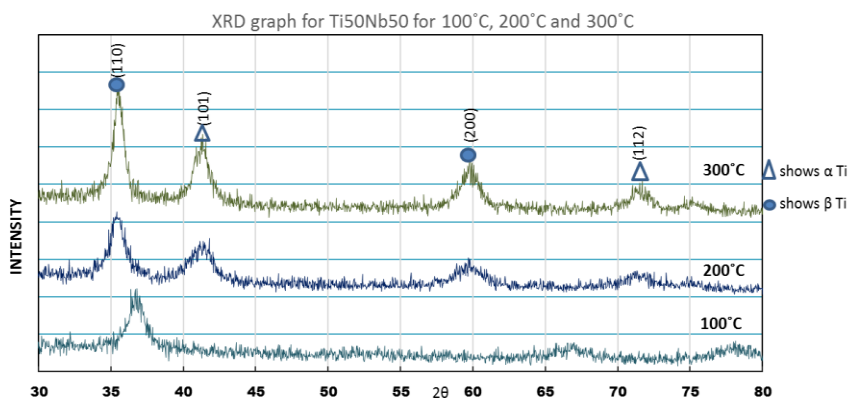

Fig.1: XRD diffraction pattern of Ti-Nb thin films

AFM:

For our samples, morphology and surface texture have been studied using AFM technique. AFM is an excellent and most common techniquewidely used in thin film characterization forstudying the surface topography at nanometric resolution that allows us to anticipate about the mechanical and surface properties of thin films [15, 16].

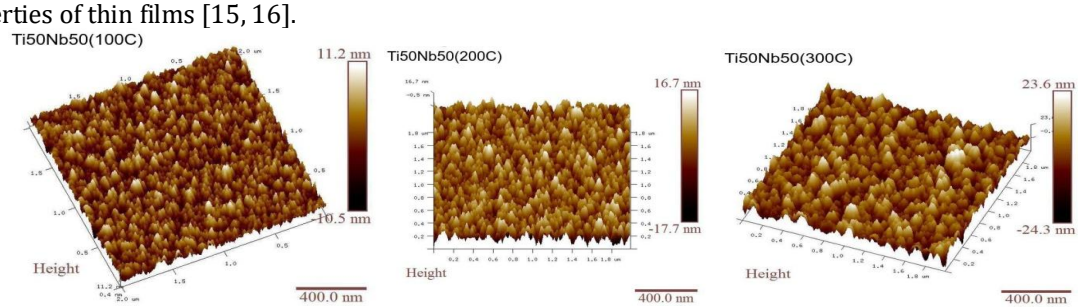

Fig.2: AFM images of Ti-Nb thin films

The AFM images depicting the morphology and roughness of Ti-Nb films deposited on glass substrates at varying temperature are shown in Fig.2. Images of alloy were taken in 5µm x 5µm area. Light brown color shows the Titanium and white color indicates Niobium. These niobium particles act as β-phase nucleation agent. With increase in temperature, more niobium and titanium particles continue to grow with consequent increase in its volume fraction in the two-phase structure. AFM images show that temperature affects the density and the size of $Ti_{50}Nb_{50}$ grains significantly. The grains have been sorted according to their size in order to determine the surface density and grain diameter of the sample. This is due to the transformation of $Ti_{50}Nb_{50}$ from the amorphous to poly crystalline phase, which involves the coalescence of smaller particles into bigger ones. AFM results are in good agreement with XRD findings, which shows the dependence of structural changes on substrate temperature. So with combination of nano particles to become large particles results increase in grain boundaries.

To further look into the surface characteristics of the synthesized samples, we have calculated the roughness using the AFM data. The roughness can be analytically described by various roughness parameters. Each sample was analyzed at five randomly chosen locations. Different parameters of roughness of all five samples for scanning areas of 2µm x 2µm and 5µm x 5µm are listed in Table 3 and Table 4 respectively. Clearly, the roughness parameter Ra increases from 2.48 nm to 5.20 nm for 2µm x 2µm scanning area and from 2.53 nm to 5.30 nm for 5µm x 5µm area with increase in temperature. Another important roughness parameter Rq also increases from 3.11 nm to 6.63 nm for 2µm x 2µm scanning area and from 3.20 nm to 6.66 nm for 5µm x 5µm scanning area. Therefore, as the temperature increases, roughness of the samples is found to increase.

Table 3: Results of different parameters of roughness of alloy $Ti_{50}Nb_{50}$at 2µm x 2µm

Alloy composition / Results	Image Rq	Image Ra	Image Rmax	Rz	Rp
100°C	3.11nm	2.48nm	24.1nm	25.9nm	12.9nm
200°C	4.86nm	3.85nm	42.2nm	48.5nm	24.2nm
300°C	6.63nm	5.20nm	61.9nm	70.5nm	35.3nm

Table 4: Results of different parameters of roughness of alloy $Ti_{50}Nb_{50}$ at 5µm x 5µm

Alloy composition / Results	Image Rq	Image Ra	Image Rmax	Rz	Rp
100°C	3.20nm	2.53nm	33.8nm	44.8nm	22.4nm
200°C	4.96nm	3.95nm	51.9nm	60.1nm	30.1nm
300°C	6.66nm	5.30nm	54.8nm	57.1nm	28.6nm

SEM AND EDX:

We have recorded the FESEM micrographs of all the samples as shown in Fig. 3. Evidently, it enables us to further look into the microstructural features of the samples synthesized. FESEM micrographs clearly shows that change of microstructure of $Ti_{50}Nb_{50}$ thin films deposited at 100°C, 200°C and 300°C.

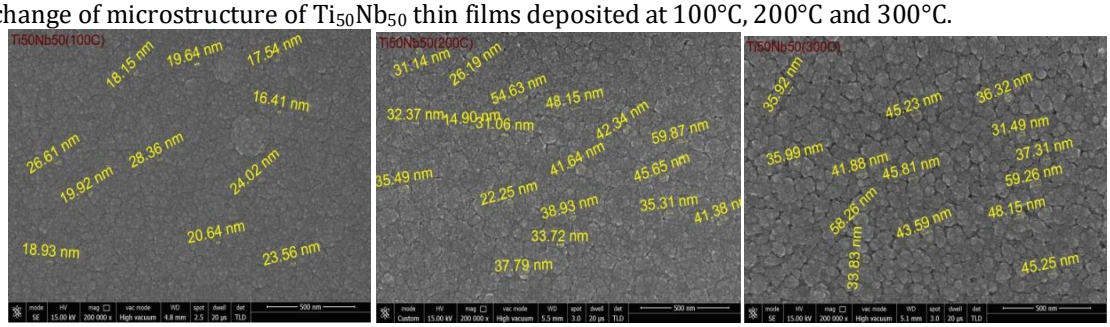

Fig.3: SEM images of Ti-Nb thin films

Grain size of the films was calculated using FESEM images by using the average formula. The calculated values of grain sizes for $Ti_{50}Nb_{50}$ alloy at 100, 200, 300°C are 20.50, 35.90 and 46.06 nm respectively. The grain sizes for all these samples were also calculated from online software **Image J** with images of 200k magnification. Grain size for Ti50Nb50 at 100°C is 21nm, at 200°C grain size is 35.50 nm and at 300°C grain size is 45 nm. From the grain size analysis we can say that size of the grain increases from 20.50 nm to 46.06 nm with the increase in temperature from 100°C to 300°C. The morphology of grain changes and becomes denser due to the higher surface and bulk diffusivity of sputtered atoms.

The Nb particles are found to be of white color and Ti particles are of dark grey color in the micrographs. It is evident from the Fig 3 that $Ti_{50}Nb_{50}$alloy has columnar structure with voids and boundaries throughout the film thickness. Clearly with the increase in temperature, the grain size increase as evident from bigger boundaries visible in the micrographs. These findings are in agreement with the results of XRD.

The EDX is used to acquire surface compositions of these films. Typical EDX spectra and corresponding composition results of the $Ti_{50}Nb_{50}$ are shown in Fig 4 and Table 5 respectively. The chemical compositions of all the samples i.e. the Ti and Nb percentages as determined from EDX analysis validate the compositions of samples.

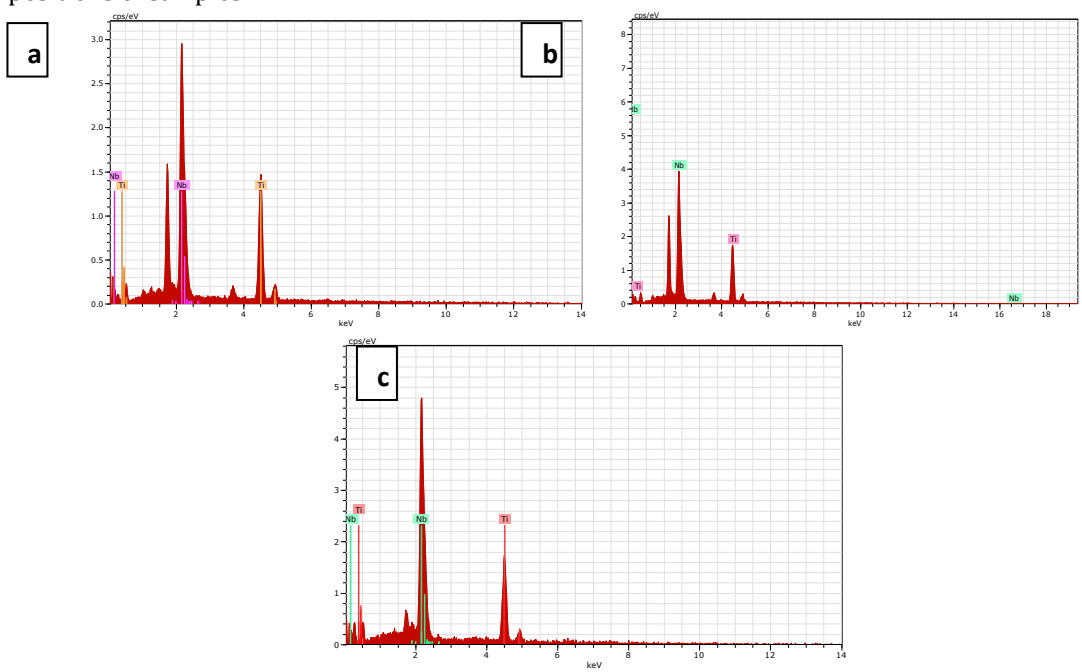

Fig.4: EDX graphs of Ti-Nb thin films (a) 100°C, (b) 200°C and (c) 300°C

Table 5: Composition of Ti-Nb elements in $Ti_{50}Nb_{50}$ alloy

Temprature	Element	Atomic Number	[wt.%]	[at.%]
100°C	Niobium	41	69.43	53.92
	Titanium	22	30.57	46.08
200°C	Niobium	41	69.22	53.73
	Titanium	22	30.78	46.27
300°C	Niobium	41	68.90	53.50
	Titanium	22	31.10	46.50

Hall Effect Measurements:

Many factors are known to influence the electrical resistivity of metals like chemical composition, atomic structure, phase changes, grain size, temperature and pressure. The change in the electrical resistivity of the $Ti_{50}Nb_{50}$ films could be mainly attributed to the difference in microstructural evolution. The film deposited at 100°C displayed a smaller and less densely packed grain microstructure with open boundaries and formation of more voids due to the fact that the Ti and Nb particles have a longer free pathway and a higher kinetic energy during deposition, which makes the less number of grain boundaries and increased the carrier mobility, resulted in a lower electrical resistivity as in Table 6. As substrate temperature increases from 100°C to 300°C, the presence of intergranular voids and porous structure in the $Ti_{50}Nb_{50}$ film was caused by the lower kinetic energies of $Ti_{50}Nb_{50}$ particles during deposition, which led to a higher electrical resistivity. Similar results were also observed in the AFM and SEM, which revealed the increase in grain size and roughness of the $Ti_{50}Nb_{50}$ film on the glass substrates with increase in temperature from 100°C to 300°C. The carrier mobility values of the $Ti_{50}Nb_{50}$ thin films, as obtained from Hall Effect measurement, are

listed in Table 6. The carrier mobility dropped with the increasing temperature during deposition, which confirms the characteristic variation of electrical resistivity observed in the fabricated films.

Table 6: Resistivity, Carrier Mobility and Conductivity $Ti_{50}Nb_{50}$ alloy at different temperature

Temperature	Resistivity	Carrier Mobility	Conductivity
100°C	2.39×10^{-4}	2.64×10^{-1}	$4.18 \times 10^{+3}$
200°C	3.51×10^{-4}	7.98×10^{-2}	$2.85 \times 10^{+3}$
300°C	3.99×10^{-4}	3.50×10^{-2}	$2.51 \times 10^{+3}$

CONCLUSION:

Niobium rich Titanium based thin films with nominal composition $Ti_{50}Nb_{50}$ have been successfully prepared on glass substrate at different substrate temperature (100°C, 200°C and 300°C) by RF magnetron sputtering. Structural and electrical properties of the thin films were investigated by XRD, AFM and FESEM analysis. At 100°C, films are found to be prominently amorphous and with increase in substrate temperature, these films are becoming polycrystalline and the grain size is found to show a direct dependence on the substrate temperature. AFM images established the formation of nanostructure thin films and the surface roughness of these films is found to increase from 2.48nm to 5.20nm for area 2μm x 2μm and 2.53nm to 5.30nm for 5μm x 5μm area with increasing substrate temperature from 100°C to 300°C. SEM images showed the increase in grain size as a function of substrate temperature; from 20.50nm for 100°C to 46.06nm for 300°C. EDX results validate the composition of the films. Hall effects measurements showed a characteristic trend of variation in electrical properties of the films; both mobility and electrical resistivity of the films are found to increase with the increase in substrate temperature.

CONFLICT OF INTEREST: None

ACKNOWLEDGEMENT: Authors acknowledge Punjab Technical University, Kapurthala, MNIT Jaipur and SBSSTC Ferozpur for directly or indirectly contributing to successful completion of this work.

REFERENCES:

1. A.A.Volinsky, J.Vella, I.S.Adhihetty, Mater.Res.Soc.Symp.649, Q5.3.1-Q5.3.5., (2001).
2. A.Radisic, O.Luhn, H.G.G Phiplisen, Microelectronics Engineering, (2010), Article in press.
3. J.L.Mermet, M.J.Mouche, F.Pires, J.Phys. IV 05(C5) (1995)517.
4. N.Nevolin, A.V.Zenkevich, X.Ch.Lai, Laser Physics 11(7), (2001)824.
5. S.B. Ogale, T.V. Venkatesan, M.G. Blamire, Functional Metal Oxides: New Science and Novel Applications, Wiley-VCH Verlag GmbH & Co, 2013.
6. K. Wasa, I. Kanno, H. Kotera, Handbook of Sputtering Technology, William Andrew Books – Elsevier, 2012.
7. D.R.Gibson, I.T.Brinkley, E.M.Waddell, Society of Vacuum Coaters 151(505), (2008)856.
8. P.J. Bania, D. Eylon, R.R. Boyer, D.A. Koss (Eds.), Titanium Alloys in the 1990's, The Mineral, Metals & Materials Society, Warrendale, PA, (1993)3–14.
9. L. Wang, L.Meng, V.Teixeira, S.Song, Z.Xu, X Xu, "Structure and optical properties of ZnO:V thin films with different doping concentration", Thin Solid Films 517, (2009)3721-3725.
10. File PD. Joint committee on powder diffraction standards. ASTM, Philadelphia, Pa. 1967:9-185.
11. Han MK, Kim JY, Hwang MJ, Song HJ, Park YJ. Effect of Nb on the microstructure, mechanical properties, corrosion behavior, and cytotoxicity of Ti-Nb alloys. Materials. 2015 Sep 9;8(9):5986-6003.
12. R.W. Schutz, D. Eylon, R.R. Boyer, D.A. Koss (Eds.), Beta Titanium Alloys in the 1990's, The Mineral, Metals & Materials Society, Warrendale, PA, (1993) 75–91.
13. S.K. Sharma, H.S. Vijaya, S. Mohan, Physics Procedia 10 (2010) 44–51.
14. A. Kumar, S.K. Sharma, S. Bysakh, S.V.Kamat, S. Mohan, Journal of Materials Sciences & Technology 26 (11) (2010) 961–966.
15. N. Jalili and K. Laxminarayana, "A review of atomic force microscopy imaging systems: application to molecular metrology and biological sciences," Mechatronics, vol. 14, no. 8(2004)907–945.
16. M. Kwoka, L. Ottaviano, and J. Szuber, "AFM study of the surface morphology of L-CVD SnO2 thin films," Thin Solid Films, vol. 515, no. 23, (2007)8328–8331.